Conclusions

The principal advantage of the cable load over commercial loads is its much greater linearity. Therefore, it is specifically recommended for use in systems tests where precise harmonic measurements are important. In general, a cable load is practical and even advantageous for use in the HF, VHF, and UHF frequency ranges, provided that power requirements at upper VHF and at UHF frequencies are not too high. The inherent simplicity of the cable load allows it to be more readily available than commercial loads. A considerably greater number of suppliers stock cables rather than dummy loads. The majority of cables found in the laboratory do not contain Copperweld or ferromagnetic Nichrome center conductors, and thus are suitable for linear dummy loads.

References

[1] "Engineering study for electrical hull interaction," U.S. Navy Contract N-00123-67-C-1256.
[2] W. W. Macalpine, "Computation of impedance and efficiency of transmission line with high standing-wave ratio," *AIEE Trans. (Communications and Electronics)*, vol. 72, pp. 334–339, July 1953.
[3] *Military Standardization Handbook—RF Transmission Lines and Fittings*, MIL-HDBK-216, January 4, 1962.

Predicting the Magnetic Fields from a Twisted-Pair Cable

J. RONALD MOSER, MEMBER, IEEE, AND RALPH F. SPENCER, JR., MEMBER, IEEE

***Abstract*—A theory that predicts the magnitude of low-frequency magnetic fields near a current-carrying twisted-pair cable is developed. By asymptotically expressing the theoretical results, it is shown that the magnetic fields from a twisted-pair cable of pitch distance p decrease exponentially with the radial distance from the center of the cable. The asymptotically expressed result is verified experimentally for a radial distance as large as $(3/2)p$. At such a distance, the maximum fields from the cable are shown to be 50 dB below that from a two-wire line (two parallel wires), even though both the cable and the wire line are carrying the same amount of current.**

Introduction

THE TWISTED-PAIR (twisted-wire) cable has long been used to localize stray magnetic fields of low frequency. An extensive quantitative study of low-frequency magnetic fields near a current-carrying twisted-pair cable has not appeared primarily because of the complexity of the fields. However, qualitatively, its behavior is reasonably well understood.

The need for a quantitative study of the twisted-pair cable exists. In certain situations one must decide how closely such a cable can be placed near other cables without sustaining an intolerable amount of interference. Quantitative prediction is becoming more important as systems become more complicated and space becomes scarcer.

The twisted-pair cable can be represented mathematically as a double helix, but the magnetic fields from the helix cannot be described simply. Because the current elements from the cable constitute a complicated spatial orientation, it is hard to obtain a simple useful model for such a cable. Alksne [1] did derive a model, but it utilized the following two assumptions that precluded using it for practical interference predictions.

1) The pitch distance p is much greater than the radius a of the twisted pair. (This assumption was used to justify neglecting the r and θ components of the current and hence the z component of the magnetic field. However, experimental results have shown that a significant z component of the magnetic field exists for a twisted-pair cable.)

2) The distance from the axis of the twisted-pair cable r is much greater than a. (This condition is not necessarily true in practice.)

Manuscript received January 10, 1968. This study was made by J. R. Moser under USL Project 1-910-00-00, Navy Subproject and Task SF 013 1504-2114, and by R. F. Spencer, Jr., under Bureau of Ships Contract NObsr 85170, Index SF-0121 511, while he was attending the Moore School of Engineering, University of Pennsylvania, Philadelphia, Pa.

J. R. Moser was with the U.S. Navy Underwater Sound Laboratory, Fort Trumbull, Conn. He is now with Government Products Division, Texas Instruments, Inc., Dallas, Tex.

R. F. Spencer, Jr., was with the Moore School of Engineering, University of Pennsylvania. He is now with the Semiconductor Components Division, Texas Instruments, Inc., Dallas, Tex.

It is the purpose of this paper to provide a method without limiting assumptions for a more accurate calculation of the magnetic fields from a twisted-pair cable and to verify these fields experimentally.

Theory of the Twisted-Pair Cable

A realistic model for a twisted-pair cable is an infinitely long bifilar helix[1] (Figs. 1 and 2) that consists of two helices having the same radius and pitch; the helices are located 180 spatial degrees from each other. The electromagnetic fields for a single helix of infinite extent have been calculated by Sensiper [2]. In his calculations, he assumed that: 1) the helical wire can be represented by an infinitesimally thin current element, and 2) the effect of insulation on the wire was negligible. Both assumptions are not limiting at the low frequencies of interest here.

When Sensiper's[2] calculations are followed, the magnetic vector potential at low frequencies for the first helix $\boldsymbol{A}_1$ in a cylindrical coordinate system is

$$\begin{aligned}\boldsymbol{A}_1(r,\theta,z) = \frac{\mu_0 i \cot\Psi}{4\pi}\sum_{m=-\infty}^{\infty}\Bigg\{-j\boldsymbol{a}_r\Bigg[I_{m-1}(\eta_m)K_{m-1}\left(\eta_m\frac{r}{a}\right)\\ - I_{m+1}(\eta_m)K_{m+1}\left(\eta_m\frac{r}{a}\right)\Bigg]\\ + \boldsymbol{a}_\theta\Bigg[I_{m-1}(\eta_m)K_{m-1}\left(\eta_m\frac{r}{a}\right)\\ + I_{m+1}(\eta_m)K_{m+1}\left(\eta_m\frac{r}{a}\right)\Bigg]\\ + \boldsymbol{a}_z\Bigg[2\tan\Psi I_m(\eta_m)K_m\left(\eta_m\frac{r}{a}\right)\Bigg]\Bigg\}\\ \cdot e^{im[\theta-(2\pi/p)z]},\quad r>a \qquad (1)\end{aligned}$$

where

a = helix radius

$\cot\Psi = \dfrac{2\pi a}{p} = q$

i = helix current

$I_m(X)$, $K_m(X)$ = mth order modified Bessel functions of first and second kinds, respectively

p = helix pitch distance

r = radial distance from axis of twisted-pair cable

$\eta_m = |m\cot\Psi| = |mq|$

μ_0 = free space permeability

Ψ = helix pitch angle.

[1] This model was suggested by Dr. M. Kaplit, Moore School of Electrical Engineering, University of Pennsylvania, in a private communication.

[2] Sensiper calculated the Hertzian electric potential instead of the magnetic vector potential.

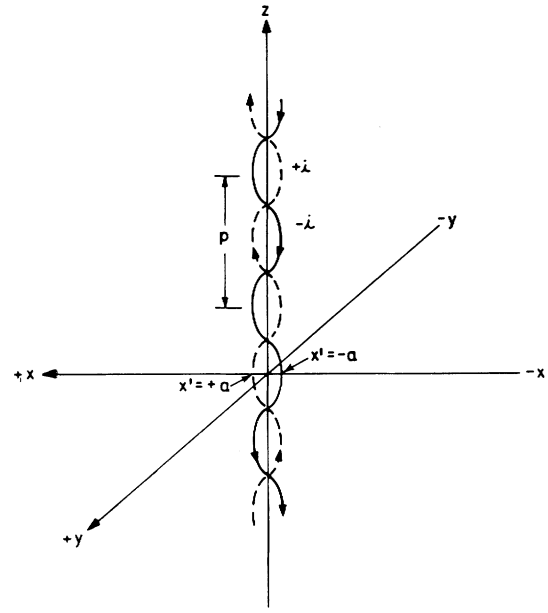

Fig. 1. Bifilar helix model of twisted-pair cable. a—helix radius; p—helix pitch distance.

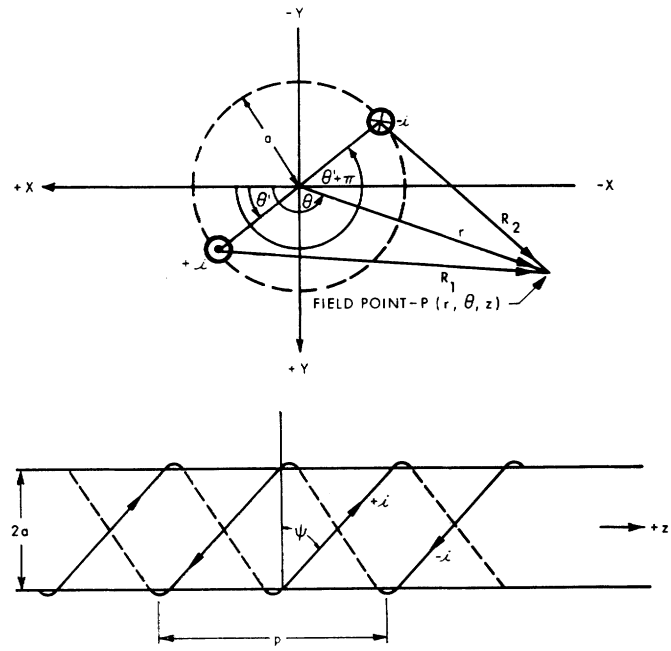

Fig. 2. Top and side views of bifilar helix model. a—helix radius; $\cot\Psi = 2\pi a/p$; p—helix pitch distance; Ψ—helix pitch angle.

The magnetic vector potential for the second helix $\boldsymbol{A}_2$ can be derived from $\boldsymbol{A}_1(r,\theta,z)$ by substituting $-i$ for $+i$ and by replacing θ by $\theta \pm \pi$ (or, equivalently, replacing z by $z \pm (p/2)$). Mathematically, this procedure corresponds to the one used in the following equation:

$$\begin{aligned}\boldsymbol{A}_2(r,\theta,z) &= -\boldsymbol{A}_1(r,\theta\pm\pi,z)\\ &= -\boldsymbol{A}_1\left(r,\theta,z\pm\frac{p}{2}\right).\end{aligned} \qquad (2)$$

The total magnetic vector potential produced by the bifilar helix current is $\boldsymbol{A}_T = \boldsymbol{A}_1 + \boldsymbol{A}_2$. Since $\eta_{-m} = \eta_m$, $I_{-n}(X) = I_n(X)$, and $K_{-n}(X) = K_n(X)$, $\boldsymbol{A}_T = \boldsymbol{a}_r A_{T_r} + \boldsymbol{a}_\theta A_{T_\theta} + \boldsymbol{a}_z A_{T_z}$, where

$$A_{T_r} = \frac{\mu_0 i \cot \Psi}{\pi} \sum_{m=0}^{\infty} \left[I_{2m}(\eta_{2m-1}) K_{2m}\left(\eta_{2m+1}\frac{r}{a}\right) - I_{2(m+1)}(\eta_{2m+1}) K_{2(m+1)-1}\left(\eta_{2m+1}\frac{r}{a}\right)\right] \cdot \sin\left[(2m+1)\left(\theta - \frac{2\pi z}{p}\right)\right], \quad r > a \tag{3}$$

$$A_{T_\theta} = \frac{\mu_0 i \cot \Psi}{\pi} \sum_{m=0}^{\infty} \left[I_{2m}(\eta_{2m-1}) K_{2m}\left(\eta_{2m+1}\frac{r}{a}\right) + I_{2(m+1)}(\eta_{2m+1}) K_{2(m+1)-1}\left(\eta_{2m+1}\frac{r}{a}\right)\right] \cdot \cos\left[(2m+1)\left(\theta - \frac{2\pi z}{p}\right)\right], \quad r > a \tag{4}$$

and

$$A_{T_z} = \frac{2\mu_0 i}{\pi} \sum_{m=0}^{\infty} \left[I_{2m+1}(\eta_{2m-1}) K_{2m-1}\left(\eta_{2m+1}\frac{r}{a}\right)\right] \cdot \cos\left[(2m+1)\left(\theta - \frac{2\pi z}{p}\right)\right], \quad r > a. \tag{5}$$

The magnetic-field components are found from $\boldsymbol{B} = \nabla \times A_T$, which yields the following results:

$$B_r = -\left(\frac{\mu_0}{\pi p}\right) \sum_{m=0}^{\infty} 2(2m+1) \left\{ \left[\frac{(p/a)}{(r/a)}\right] I_{2m+1}(\eta_{2m+1}) \cdot K_{2m+1}\left(\eta_{2m+1}\frac{r}{a}\right) + \pi \cot \Psi \left[I_{2m}(\eta_{2m+1}) \cdot K_{2m}\left(\eta_{2m+1}\frac{r}{a}\right) + I_{2(m+1)}(\eta_{2m+1}) K_{2(m+1)}\left(\eta_{2m+1}\frac{r}{a}\right)\right]\right\} \cdot \sin\left[(2m+1)\left(\theta - \frac{2\pi}{p} z\right)\right], \quad r > a \tag{6}$$

$$B_\theta = -\frac{\mu_0 i}{\pi p} \sum_{m=0}^{\infty} \left\{ (2m+1) 2\pi \cot \Psi \left[I_{2m}(\eta_{2m+1}) \cdot K_{2m}\left(\eta_{2m+1}\frac{r}{a}\right) - I_{2(m+1)}(\eta_{2m+1}) K_{2(m+1)}\left(\eta_{2m+1}\frac{r}{a}\right)\right] + 2 I_{2m+1}(\eta_{2m+1}) \left[-\frac{\eta_{2m-1}}{(a/p)} K_{2m-1}\left(\eta_{2m+1}\frac{r}{a}\right) + \frac{(2m+1)(p/a)}{(r/a)} K_{2m-1}\left(\eta_{2m-1}\frac{r}{a}\right)\right]\right\} \cdot \cos\left[(2m+1)\left(\theta - \frac{2\pi}{p} z\right)\right], \quad r > a \tag{7}$$

and

$$B_z = \frac{\mu_0 i}{\pi p} \sum_{m=0}^{\infty} \cot \Psi \left\{ \frac{(p/a)}{(r/a)} \left[I_{2m}(\eta_{2m+1}) K_{2m}\left(\eta_{2m-1}\frac{r}{a}\right) + I_{2(m+1)}(\eta_{2m+1}) K_{2(m+1)}\left(\eta_{2m+1}\frac{r}{a}\right)\right] + I_{2m}(\eta_{2m-1}) \cdot \left[-\frac{\eta_{2m+1}}{(a/p)} K_{2m+1}\left(\eta_{2m+1}\frac{r}{a}\right) + \frac{2m(p/a)}{(r/a)} K_{2m}\left(\eta_{2m+1}\frac{r}{a}\right)\right] + I_{2(m+1)}(\eta_{2m+1}) \cdot \left[-\frac{\eta_{2m+1}}{(a/p)} K_{2m+3}\left(\eta_{2m+1}\frac{r}{a}\right) + \frac{2(m+1)(p/a)}{(r/a)} K_{2(m+1)}\left(\eta_{2m-1}\frac{r}{a}\right)\right] - \frac{(2m+1)(p/a)}{(r/a)} \left[I_{2m}(\eta_{2m+1}) K_{2m}\left(\eta_{2m-1}\frac{r}{a}\right) - I_{2(m+1)}(\eta_{2m+1}) K_{2(m+1)}\left(\eta_{2m+1}\frac{r}{a}\right)\right]\right\} \cdot \cos\left[(2m+1)\left(\theta - \frac{2\pi}{p} z\right)\right], \quad r > a. \tag{8}$$

Calculations

A computer program was written to obtain numerical results for B_r as a function of radial distance r. The peak amplitude of B_r was seen to be an approximate exponential function of r. As r increased, the approximation became better.

The computer subroutine for calculating $I(\alpha)$ and $K(\beta)$ was limited by $\beta < 88$. For our calculations

$$\beta = (2m+1) q \frac{r}{a} = (2m+1)\frac{2\pi r}{p} < 88 \tag{9}$$

or, equivalently,

$$(2m+1) r < \frac{88 p}{2\pi}.$$

As r increased and the exponential approximation became closer, fewer terms were included in the final result. Therefore, the first term ($m = 0$) appeared to be the dominant term. We set $m = 0$ and then $\sin[\theta - (2\pi/p)z] = 1$ in (6) and used the asymptotic expression for $K(\beta)$

$$\lim_{\beta \to \infty} K_\nu(\beta) = \sqrt{\frac{\pi}{2\beta}}\, e^{-\beta}. \tag{10}$$

Thereby, a closed form was obtained for the maximum radially directed flux density

$$B_r(\max) = \frac{2\mu_0 i}{\pi} \left\{ \frac{1}{r} I_1(q) + \frac{q\pi}{p} [I_0(q) + I_2(q)] \right\} \sqrt{\frac{\pi a}{2qr}}\, e^{-(q/a)} \tag{11}$$

where the symbols are as defined in Figs. 1 and 2.

For typical values of q, i.e., $1/20 \leq q \leq 2/3$, $I_0(q)$ is the dominant term, and (11) reduces to (MKS units)

$$B_r(\max) = \frac{\mu_0 i}{\sqrt{pr}} q I_0(q) e^{-(2\pi/p)r}. \quad (12)$$

When setting $m = 0$ and then $\cos[\theta - (2\pi/p)z] = 1$ in (7) and (8), the same result applies for $B_\theta(\max)$ and $B_z(\max)$. Realizing that for $q \leq 2/3$,

$$I_0(q) = 1 + (q/2)^2 + \frac{(q/2)^4}{(2!)^2} + \frac{(q/2)^6}{(3!)^3} + \cdots \approx 1$$

and taking 20 $\log_{10}$ of both sides and arranging the terms in order of descending importance, we obtained for the maximum flux densities

$$B_{r,\theta,z}(\max) = -54.5\frac{r}{p} - 20\log_{10}\left(\frac{1}{a}\right) - 30\log_{10} p - 10\log_{10} r + 9.8 \quad (13)$$

where

a = radius of helices in inches
$B_{r,\theta,z}(\max)$ = maximum r, θ, or z directed magnetic flux density per ampere of current in decibels relative to 1 gauss
p = pitch distance of twisted-pair cable in inches
r = radial distance from axis of twisted-pair cable in inches.

From the sinusoidal multipliers in (6)–(8), it is evident that for B_θ and B_z maximum, B_r is minimum. Conversely, for B_θ and B_z minimum, B_r is maximum.

It is interesting to compare the maximum fields from the twisted-pair cable with those from a two-wire line. Rather than analyze (6)–(8) in the limit as $p \to \infty$, a much more straightforward approach exists and is presented in the Appendix. The results of this approach are

$$B_r = \frac{\mu_0 i a}{\pi(r^2 + a^2)}, \quad B_\theta = \frac{\mu_0 i a}{\pi(r^2 - a^2)}, \quad B_z = 0 \quad (14)$$

where the field values apply at the points shown in Fig. 3 and where a is the half-wire spacing, center to center, and r is the radial distance from the center of the wires.

By forming the ratio of B_r from (12) and (14), we obtained

$$\frac{B_r(\text{twisted-pair cable})}{B_r(\text{two-wire line})} \leq 2\pi^2 \left(\frac{r}{p}\right)^{3/2} e^{-(2\pi/p)r} \quad (15)$$

which is valid within 10 percent for $r > 3a$ and $q < 2/3$.

Fig. 4 is a graph of 20 $\log_{10}$ [B_r(maximum twisted-pair cable)/B_r(two-wire line)] versus the ratio of radial distance to pitch distance over the range of the variable r/p in (12), for which experimental verification has been obtained (see the following section).

To verify the numerical results, two 10-foot plastic rods were machine grooved to coincide with the model shown in Fig. 1. One rod was 1/4 inch in diameter and had a 3-inch pitch length; the other rod was 1/2 inch in diameter and had a 6-inch pitch length.

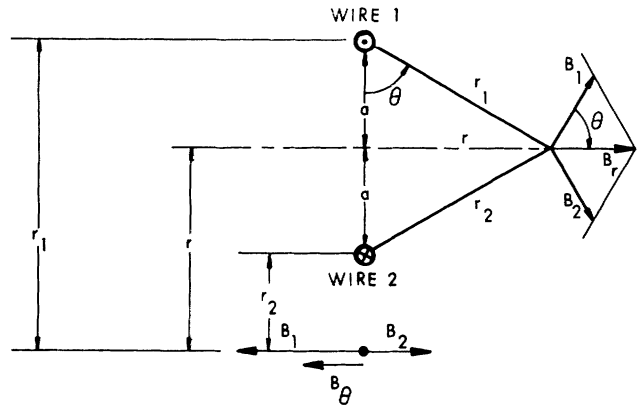

Fig. 3. Magnetic fields from two-wire line.

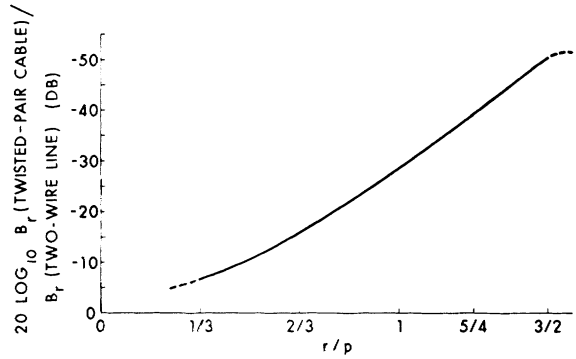

Fig. 4. Comparison of maximum radially directed flux densities from twisted-pair cable of pitch p and two-wire line.

Experimental Results

Each twisted-pair cable was formed by laying a no. 18 copper wire in each groove and then passing a known rms level sinusoidal current through the cable.

The magnetic flux density was measured with an AT-207 1/2-inch-mean-diameter loop probe coupled into a low-noise preamplifier and narrow band analyzed with a Hewlett–Packard model 302A wave analyzer. The receiving system was calibrated at each test frequency (1 to 10 kHz) with a Helmholtz coil.

Figs. 5 and 6 are plots of experimentally obtained $B_{r,\theta,z}(\max)$ versus radial distance r for each cable. Plots of (13) and (14) are included in these figures for comparison with the experimentally obtained data. The experimental data for B_r and B_z agree well (over a limited range) with (13), the asymptotically-expressed sharply truncated version of (6) and (8). Agreement between experimental data for B_θ and (13) is not so close.

Apparently, for radial distances less than one third of a pitch, the expressions for a two-wire line (14) approximate the maximum field component $B_r(\max)$ for a twisted-pair cable more closely than does (13). Of course, B_z cannot strictly be approximated in this way since it does not exist (at low frequencies) near the two-wire line. Agree-

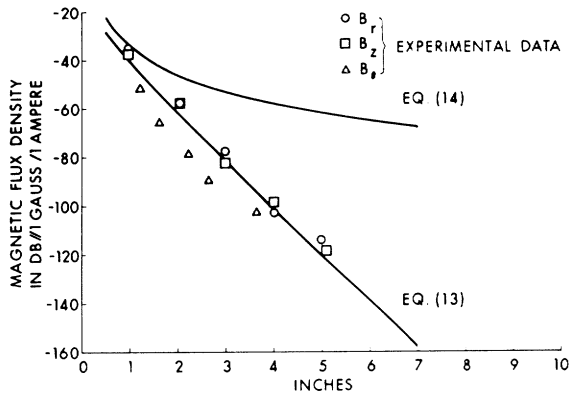

Fig. 5. Radial distance from center of twisted-pair cable, where p is 3 inches and a is $^1/_8$ inch.

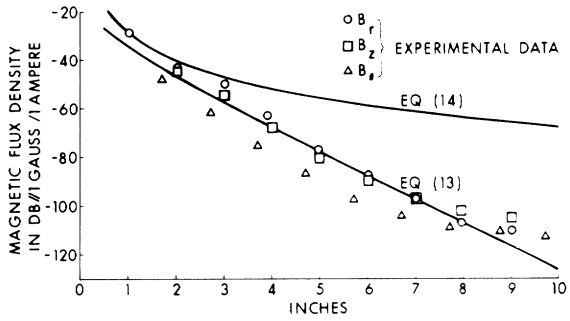

Fig. 6. Radial distance from center of twisted-pair cable, where p is 6 inches and a is $^1/_4$ inch.

ment between experimental data and data calculated for B_r and B_z from (13) is good for the following range of the variable r:

$$\frac{1}{3}p < r < \frac{3}{2}p. \tag{16}$$

Beyond this radius, the experimentally obtained field levels were generally well above the predicted levels, and the sinusoidal variation with z (or θ) no longer existed. There are three possible reasons for this (given in order of decreasing likelihood), although none of the three could be definitely established:

1) data affected more at larger radial distances by slight variations in p and a along the twisted-pair cable,

2) data contaminated by end effects,

3) spurious leakage of field from equipment or building reflections.

Possibly, since we were looking at small differences in relatively large fields, the retardation effects, which have been neglected in deriving (6)–(8) and are, in fact, extremely small in the frequency range of interest, accounted for the lack of agreement between the experimental and the theoretical results. To check this, data were obtained at 1 and 10 kHz, and it was found that differences between the theoretical and the experimental results were independent of frequency within the frequency range of interest.

The lack of agreement between experimental data for B_θ and (13) is not considered important, since B_θ (from the experimental data) is the weakest of the three components.

Conclusions

It has been shown that the maximum magnetic flux density from a twisted-pair cable decreases exponentially with radial distance from the cable according to the approximate relationship

$$B(\max) = f(\mu_0,i,q)\frac{1}{\sqrt{pr}}e^{-(2\pi/p)r}.$$

This result has been verified experimentally within a somewhat limited range for the two dominant field components B_r and B_z. The field $B(\max)$ is a critical function of p; decreasing p (tighter twist) increases the rate of field attenuation with r. At a radial distance equal to 3/2 of the pitch distance p, the maximum field levels for B_r and B_z are 50 dB below the field from a two-wire line carrying the same amount of current.

Experimental results (verified in several independent experiments) show that generally it is not possible to observe the theoretical attenuation at greater distances due to effects attributed to deviation from the theoretical model of the actual model. These deviations can be expected to be present in any practical installation.

For radial distances less than 1/3 the pitch distance p (in the region where the asymptotic expression for (6)–(8) becomes invalid), the maximum fields can be calculated by using the equations for the magnetic field from a two-wire line.

Appendix

Calculation of a Quasistatic Magnetic-Field Component Generated by a Two-Wire Line

Consider the case when $r/\lambda \ll 1$. The magnetic-field component generated by a two-wire line can be calculated using Fig. 3. For a single wire at quasistatic frequencies

$$\oint \boldsymbol{H}\cdot d\boldsymbol{l} = i$$

$$H = \frac{i}{2\pi r}.$$

Calculation of B_r

By the rules of vector addition, it can be seen that

$$B_r = 2B_1\cos\theta$$

but

$$\cos\theta = \frac{a}{(a^2 + r^2)^{1/2}}.$$

Therefore,

$$B_1 = \frac{\mu_0 i}{2\pi r_1} = \frac{\mu_0 i}{2\pi}(r^2 + a^2)^{-1/2}$$

and

$$B_r = \frac{\mu_0 i a}{\pi(r^2 + a^2)}. \tag{17}$$

Calculation of B_θ

By the rules of vector addition, it can be seen that

$$B_\theta = B_2 - B_1 = \frac{\mu_0 i}{2\pi}\left(\frac{1}{r_2} - \frac{1}{r_1}\right) = \frac{\mu_0 i}{2\pi}\frac{r_1 - r_2}{r_1 r_2}$$

and when $r_1 - a = r = r_2 + a$, we find that

$$B_\theta = \frac{\mu_0 i a}{\pi(r^2 - a^2)}. \tag{18}$$

Acknowledgment

The authors are indebted to R. M. Showers of the Moore School of Electrical Engineering, University of Pennsylvania, for his technical assistance and for his coordination of their efforts on this study, and to D. W. Counsellor of the U.S. Navy Underwater Sound Laboratory, for the computer work.

References

[1] A. Y. Alksne, "Magnetic fields near twisted wires," *IEEE Trans. Space Electronics and Telemetry*, vol. SET-10, pp. 154–158, December 1964.

[2] S. Sensiper, "Electromagnetic wave propagation on helical conductors," M.I.T. Research Laboratory of Electronics, Cambridge, Mass., Tech. Rept. 194, AD 194313, May 16, 1951.

Contributors

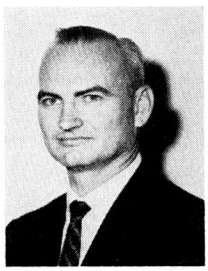

William E. Cory (M'55–SM'58) received the B.S. degree in electrical engineering from Texas A&M University, College Station, in 1950 and the M.S. degree in engineering from the University of California, Los Angeles, in 1959. He has pursued additional graduate work at Trinity University.

He joined the U. S. Air Force Security Service in 1950, where he served as a systems engineer, commissioned officer, and supervisory electronic engineer until 1957. He then joined Lockheed Aircraft Corporation, Burbank, Calif., and Marietta, Ga., where he served as an electronic systems engineer and as an aircraft development engineer specialist. In 1959 he joined the staff of Southwest Research Institute, San Antonio, Tex., as a Senior Research Engineer. There he has been active in research and development in communications, limited warfare, data processing, and electromagnetic interference fields, and is currently Director of the Electronic Systems Research Department.

Mr. Cory is a member of the Armed Forces Communication and Electronics Association, the Pattern Recognition Society, a past Chairman of the Central Texas Chapter of the IEEE G-EMC, and is a Registered Professional Engineer in the State of Texas.

✣

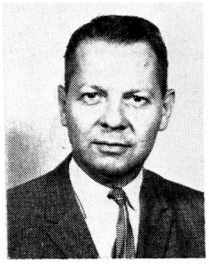

Walter C. Dolle (S'49–A'53–M'58–SM'59) received the B.S. degree from the U. S. Military Academy, West Point, N. Y., in 1939, the M.S. degree from the University of Michigan, Ann Arbor, in 1949, and did additional graduate work in electronics engineering at the University of California, Berkeley, from 1951 to 1952.

He served with the U. S. Army Signal Corps until his retirement in 1960 in the grade of Colonel. Shortly thereafter he joined the staff of Page Communications Engineers, Inc., Washington, D. C., where he participated in projects concerning an experimental passive satellite communications link and instrumentation and operation of experimental tropospheric scatter and high-frequency radio links. In 1962 he joined the staff of Southwest Research Institute, San Antonio, Tex., as a Senior Research Engineer in the Department of Electronic Systems Research. He has been engaged in work concerning radio frequency interference measurements and suppression, and is currently Manager of the Electromagnetic Compatibility Section.

Mr. Dolle is current Secretary of the Central Texas Chapter of the IEEE G-EMC.

✣

Raymond F. Elsner (S'49–A'53–M'59) was born in Chicago, Ill., on July 1, 1922. He received the B.S.E.E. degree in 1953 from the University of Illinois, Urbana.

He was employed by Motorola, Inc. from 1953 to 1962. During this period he worked